NATURAL RESOURCES PROGRAM

SPACE APPLICATIONS PROGRAMS

TECHNICAL LETTER NASA-33

U.S. Geological Survey
Department of the Interior

UNITED STATES
DEPARTMENT OF THE INTERIOR
GEOLOGICAL SURVEY
WASHINGTON, D.C. 20242

Technical Letter
NASA-33
April 1966

Dr. Peter C. Badgley
Chief, Natural Resources Program
Office of Space Science and Applications
Code SAR, NASA Headquarters
Washington, D.C. 20546

Dear Peter:

Transmitted herewith are 3 copies of:

TECHNICAL LETTER NASA-33

GEOLOGICAL STUDIES OF THE EARTH AND PLANETARY SURFACES OF ULTRAVIOLET ABSORPTION AND STIMULATED LUMINESCENCE*

by

William R. Hemphill**

and

Roger Vickers***

Sincerely yours,

William A. Fischer
Research Coordinator for
USGS/NASA Natural Resources Program

*Work performed under NASA Co -146-09-020-006
**U.S. Geological Survey, Washington, D.C.
***IITRI, Chicago, Illinois

UNITED STATES

DEPARTMENT OF THE INTERIOR

GEOLOGICAL SURVEY

TECHNICAL LETTER NASA-33

GEOLOGICAL STUDIES OF THE EARTH AND PLANETARY SURFACES OF ULTRAVIOLET ABSORPTION AND STIMULATED LUMINESCENCE*

by

William R. Hemphill**

and

Roger Vickers***

April 1966

These data are preliminary and should not be quoted without permission

Prepared by the Geological Survey for the National Aeronautics and Space Administration (NASA)

*Work performed under NASA Contract No. R-146-09-020-006

**U.S. Geological Survey, Washington, D.C.

***IITRI, Chicago, Illinois

CONTENTS

ILLUSTRATIONS

TABLES

APPENDICES

UNITED STATES
DEPARTMENT OF THE INTERIOR
GEOLOGICAL SURVEY

Technical Letter
NASA - 33
April 1966

GEOLOGICAL STUDIES OF THE EARTH AND PLANETARY SURFACES BY ULTRAVIOLET ABSORPTION AND STIMULATED LUMINESCENCE

by

William R. Hemphill
and
Roger Vickers

SUMMARY

Laboratory and field studies by the U.S. Geological Survey and by the IIT Research Institute, are being conducted to determine significance of ultraviolet spectral reflectance and stimulated emission measurements in discriminating between surface features and materials, initially from aircraft altitudes, and later from earth and lunar orbit. Hopefully, these studies will lead to proposals for participation in specific space flights.

To date the laboratory studies have included ultraviolet reflectance and emission measurements of common rocks and rock-forming minerals at wavelengths as short as 2200Å. These studies suggest that although less energy is reflected by some natural materials in the ultraviolet than in the visible region of the spectrum, contrast for some materials imaged at 2500Å exceeds image contrast of the same materials at longer wavelengths. This work is continuing and recently was extended into the vacuum ultraviolet The interaction of this region of the spectrum with rocks and other natural materials is poorly known. Some of the higher intensity solar emission lines in the vacuum ultraviolet, for example, Lyman $\underline{a}$ at 1216Å, may be especially meaningful in studies of the lunar surface from orbital altitudes.

Preliminary airborne tests with an optical-mechanical line-scanner equipped with an ultraviolet-sensitive photomultiplier detector have yielded long-wavelength ultraviolet imagery of a number of geologic and agricultural test sites in the NASA remote sensor evaluation program. Results of some of these tests, conducted from altitudes up to 15,000 feet, have been encouraging and additional high altitude imaging tests are planned using experimental data reduction and image enhancement techniques to compensate, in part, for excessive atmospheric attenuation in the ultraviolet.

Ground and aircraft tests of a high resolution spectrometer are also planned in an attempt to detect ultraviolet stimulated luminescence of natural features by means of the "Fraunhofer line-depth method". This

method, in which the central intensity of a Fraunhofer line observed in the solar spectrum directly is compared with its earth-reflected conjugate, has already been used successfully by astronomers with earth based instruments to detect lunar luminescence against a high solar background.

Preliminary studies have been completed by IIT Research Institute, Chicago, outlining major constructional and operational constraints of suitable imaging and spectrometer systems for detecting ultraviolet reflectance and luminescence of terrestrial and lunar materials from orbital altitude. These studies are encouraging; they indicate that suitable space-flight hardware could be built relatively quickly using off-the-shelf components and without an elaborate development program. Moreover, both reflectance and emission functions will be integrated into a single package, sharing the same fore optics and spacecraft window. Both imaging and spectral scans could be achieved electronically, thereby completely eliminating problems of mechanically moving parts in a launch and space environment. It is estimated that the integrated package would weigh less than 150 pounds, occupy less than five cubic feet, and require less than 50 watts of power. The package could be virtually self-contained with a minimum interface with other experiments or spacecraft functions.

Field of Investigation

Study of ultraviolet absorption and luminescence properties of selected natural features on the surface of the earth, moon, and planets from orbital platforms, through the use of integrated ultraviolet and visible imaging and spectrometer systems.

Principal Investigator

William R. Hemphill, U.S. Geological Survey

Co-Investigators

Frank Senftle, U.S. Geological Survey, Washington, D. C. Roger Vickers, IIT Research Institute, Chicago, Illinois. Victor I. Meyers, U.S. Department of Agriculture, Weslaco, Texas. Additional co-investigators from other fields, possibly including geography, meteorology, marine biology, oceanography, are to be selected.

OBJECTIVES To study the ultraviolet spectrum in terms of its application in discriminating and identifying geologic features on the surface of the earth, moon, and other planetary bodies. Study is a three-phase program consisting of:

* Ground-based feasibility studies.

* Aircraft data collection and analysis.

* Spacecraft experiment design and operation.

Phases I and II have been started. In detail, the program is outlined as follows:

Laboratory and field studies to develope preliminary data interpretation and instrument calibration techniques.

1. Laboratory studies of ultraviolet reflection and stimulated luminescence of terrestrial and meteoritic materials.

2. Field studies to determine the interaction of solar ultraviolet energy with natural materials in situ, using both ground-based and aircraft instruments.

B. Collection of ultraviolet reflectance and stimulated luminescence data from earth orbital altitudes.

1. To discriminate geologic and terrain features by:

a. measurement of relatively high reflectivities of selected surface materials in the ultraviolet at wavelengths longer than 3500Å.

c. delineation of geologic and terrain features by correlation of the above data with those data obtained by other detectors operating at longer wavelengths.

To evaluate instrumentation, performance, spacecraft integration, data reduction and interpretation techniques from earth orbit prior to lunar and planetary orbital flights.

C. Collection of ultraviolet reflectance and luminescence data from lunar orbital altitudes.

1. To discriminate geologic and lunar terrain features by:

a. measurement of significant differences in their abilities to reflect solar ultraviolet energy (<1500Å - 3000Å).

b. measurement of stimulated luminescence that may be exhibited in the ultraviolet or visible regions of the spectrum due to stimulation by solar electromagnetic and corpuscular radiation.

2. To correlate above data with data obtained by sensors operating in other parts of the spectrum (visible, IR, microwave, etc.), both from orbit and on the surface, in an attempt to determine gross surface composition of as large a part of the lunar surface as is permitted by orbital configuration.

Supporting Considerations

A. Ultraviolet spaceflight experiment will be composed of both spectrometer and imaging systems integrated into a single package, using a single part and one set of fore-optics, weighing less than 150 pounds, and occupying less than five cubic feet.

B. Components of both the imaging and the spectrometry systems are available as off-the-shelf components; hence, the prototype design does not require an extensive developmental program.

C. Both imaging and spectral scans are achieved electronically, thereby eliminating operational problems of mechanically moving parts in a launch and space environment.

D. Although the emission spectormeter is designed primarily for detection of Fraunhofer lines, the instrument serves a dual function in that it will also provide reflectivity data throughout parts of the ultraviolet and visible regions of the spectrum.

E. In both earth and lunar orbital experiments, relatively detailed ultraviolet imagery will be obtained by means of the narrow field (5^{0}), high magnification optical system, thus complementing the wide field-of-view imagery obtained by means of the multi-spectral (UV, visible, IR) imaging radiometers which is being considered by other experimenters.

F. In the lunar experiment, ultraviolet imagery obtained by electronic line-scan techniques, will complement the photographic multispectral experiments, but at shorter wavelengths where effectiveness of film is reduced.

JUSTIFICATION

Luminescence

Ultraviolet-stimulated luminescence is a property that has been used as an aid in detecting and discriminating between some natural materials. Small hand-carried ultraviolet lamps have been used for many years in the exploration for luminescing minerals such as scheelite (CaWO), an ore of tungsten. However, these portable ultraviolet sources are low powered and are rarely effective more than a few feet from the outcrop. The work must be conducted at night in order to avoid obscuring the ultraviolet stimulated luminescence by a daytime high solar background. Moreover, ultraviolet sources commonly used are line emitters and may be incapable of stimulating luminescence by means of their continuum where their output is low. Thus, an ultraviolet line source such as mercury, which emits strongly at 3663Å, probably would not be able to stimulate luminescence of a mineral or natural material whose excitation wavelength was, say 3690Å. The sun emits as a nearly continuous source; however, detecting luminescence during daylight is difficult; eclipsing methods are inadequate because they presuppose that phosphorescence is longer than the period of excitation. Heretofore, these operational problems have reduced the application of ultraviolet-stimulated luminescence as prospecting tool.

Recently, Kozyrev (in Kopal, 1962), Dubois (in Kopal, 1962), and Spinrad (1964) used a suitable technique for detecting luminescence on the lunar surface by means of earth-based spectrometers. Briefly, this method involves observing the ratio of the central intensity of selected Fraunhofer lines to the continuum in the ultraviolet and visible spectrum as reflected from the lunar surface, and comparing it with the central intensity of the same lines observed in the solar spectrum directly. Luminescence is indicated where the ratio of the central intensity of a specific Fraunhofer line to the continuum in a reflected lunar spectrum is lower than its solar conjugate (fig. 1). Table I shows some luminescent intensities of several regions on the lunar surface which Dubois (in Kopal, 1962) measured by the Fraunhofer "line depth method". According to Dubois, the intensity of the lunar luminescence varied between three and 25 per cent.

It is proposed that this technique may be feasible for detection of materials on the earth's surface which have been stimulated to luminesce by the solar ultraviolet at wavelengths longer than 3000Å. A spectrometer designed to scan appropriate Fraunhofer lines (Table II) in the near ultraviolet and visible regions will be used to test this technique from an aircraft. Low altitude overflights might be of use in preliminary delineation of vein or placer deposits by means of associated luminescing minerals such as zircon (Foster, 1948); or uranium and thorium minerals. High altitude aircraft and balloon flights could also be used to test the application of this technique.

If deposits of luminescing materials are well exposed and sufficiently extensive to be detected from orbital altitudes, a suitable spectrometer system could be included aboard one of the early AAP earth orbiters. Some phosphate rocks are luminescent under long-wave ultraviolet light (Hemphill and Gawarecki, 1964) and some deposits, notably those in Spanish Sahara (British Sulphur Corp., Ltd., 1961) and other parts of North Africa, cover many square miles. Phosphate, used as commercial fertilizer, is vital to the agricultural economies of several less-developed regions of the world. Discrimination of luminescent areas where phosphate is suspected to occur, could provide information of direct importance in subsequent ground exploration.

Similarly, some evaporates, including sodium carbonate, sodium sulfate, and potash deposits of alkalai playas and marine brines, are luminescent (Gleason, 1960) and are of widespread areal extent in some arid regions. Some borate minerals are commonly luminescent and extensive borax surface crusts occur in southern California, Chile, Bolivia, and Argentina (Bateman, 1942, p. 768). Oil shales are also commonly widespread and some are known to luminesce; Reicker (1962) relates the spectral response of hydrocarbon fluorescence to the distance crude petroleum has migrated from the source rock. Some marine life, including near surface floating plankton and kelp, are bio-luminescent and is of interest to marine biologists.

It is also proposed that this "line depth method" could be used for further study and discrimination of surface materials from lunar orbital altitude. Without a protective atmosphere, significant areas on the lunar surface are apparently stimulated to luminescence by direct solar ultraviolet or x-ray radiation, proton bombardment, and perhaps other agents not yet well understood. Myronova (1965), Kopal (1965, p. 37), and Lipson (1965) have suggested that luminescence properties of lunar materials may be of direct importance in determining their composition. At the very least, mapping the distribution of luminescing areas and noting time-variations in luminescent intensities, would be an important step in understanding the interrelationship of solar stimuli and specific luminescing localities on the lunar surface.

Reflected Ultraviolet Energy

Feasibility of detecting solar ultraviolet energy reflected from the earth's surface, from orbital altitudes is limited by atmospheric attenuation factors. Energy at wavelengths shorter than 2950Å is absorbed by ozone and oxygen in the atmosphere, and energy at longer wavelengths in the ultraviolet is severely scattered. Despite these problems, near ultraviolet line-scan imagery has been obtained from an aircraft from altitudes as great as 15,000 feet (fig. 2) without the use of image enhancement techniques. By using similar photoelectric devices, as well as image enhancement methods in data processing, it is believed that ultraviolet imagery can be obtained from earth orbital altitudes at wavelengths greater than 3500Å. For example, it may be possible to compensate, in part at least, for atmospheric attenuation factors through ground-based signal processing techniques during the post-flight data reduction phase. Specific atmospheric absorption and

scattering coefficients would be calculated on the basis of atmospheric conditions and ultraviolet reflectivities that prevailed and were measured in certain key areas where ground and atmospheric monitoring stations were operated during orbital overflight. These data would be used to modulate the tape output signal during imagery print-out. In addition, reflection spectra will be obtained in the long wave ultraviolet and visible region of the spectrum, in the normal course of scanning appropriate Fraunhofer lines with the emission spectrometer.

In lunar orbit, the absence of an atmosphere will permit detection of solar ultraviolet energy reflected from the lunar surface, at wavelengths as short or shorter than 1500Å. It is believed that measurements of this energy will convey information of direct importance in discriminating between lunar surface materials and in evaluation of surface texture

A spectrometer is proposed to measure the spectral distribution of ultraviolet energy reflected from the lunar surface. Most natural materials commonly show a gradual reduction in spectral reflectance with reduction in wavelength from the visible into the ultraviolet (Fischer and Gerharz, 1964; Hemphill, 1965; Watts, 1966). This is shown for four of the five specimens in figure 3. However, the shape of the spectral curve is noticeably different for each specimen.

Moreover, the relative intensity varies with wavelength; for example, rhyolite pumice is next to the brightest at wavelengths longer than 3500Å, but shows the least reflectance at 2500Å. It is not to be implied that these curves are necessarily unique for the materials shown. The curves do show, however, that measurements of spectral reflectance in the ultraviolet and visible regions of the spectrum may vary with composition and surface texture. Similar studies by Luckiesh (1946) show that although reflectivities of some mineral pigments are all near 90 per cent in the visible region, reflectivities of these materials range from six to 83 per cent near 3000Å in the ultraviolet. Dupee (1965) conducted spectral reflectance measurements on 32 rock and mineral samples in the vacuum ultraviolet. He concluded that relative values of reflected intensity at 1304Å, 1216Å, 1167Å, and 584Å were related to certain compositional elements, including silica content, iron, and magnesium. Similar spectrometer measurements of reflectance data may be useful in discriminating lunar surface materials from lunar orbital altitudes.

In addition to a spectrometer, an imaging system is proposed to selectively image those lunar surface materials with relatively high reflective coefficients in the ultraviolet. It is believed that some natural objects may display more tonal contrast when imaged by means of reflected ultraviolet energy than by visible light. In figure 3, for example, spectral reflectance in the visible region generally ranges between 20 to 30 per cent for all of the specimens and image tone would tend to be similar. At 2500Å less energy is reflected by the specimen; however, the dolomite shows more than 4x the spectral reflectance of the pumice, and other materials also show increased differences in spectral reflectance. Image contrast would be more apparent for these features imaged at 2500Å than at longer wavelengths.

Similar laboratory studies of granite, gabbro, serpentine, and quartzite, conducted by Fischer and Gerharz (1964), and Greenman, et al, (1965), also suggest that the greatest image contrast for some materials can be attained in the ultraviolet. In areas where such differences in reflectivity prevail, it should be possible to selectively image, and thereby discriminate only materials with higher reflectivity. Materials in adjacent areas where reflectivities are lower would be weakly imaged or not apparent above the noise level. Thus morphological features and surface materials of as large a part of the lunar surface as is permitted by orbital constraints will be mapped in terms of spectral reflectance characteristics in the ultraviolet.

It is expected that ultraviolet imagery and spectral reflectance data obtained from a lunar orbital platform will complement data obtained by other detecting devices operating at longer wavelengths, such as in the visible, infrared, and radar regions. Each imaging band, considered separately, will aid in discriminating between features. Collectively, all the bands will comprise a "signature" for some materials, which, hopefully, can be interpreted in terms of composition and surface texture.

PARAMETERS TO BE STUDIED

A. Aircraft

1. Ultraviolet stimulated luminescence emitted by natural materials in ultraviolet and visible regions of the spectrum at wavelengths longer than 3500Å.

2. Ultraviolet energy reflected by the earth's surface at wavelengths longer than 3500Å.

B. Earth orbit

1. Spectral distribution of ultraviolet stimulated luminescence emitted by the earth's surface in the ultraviolet and visible regions of the spectrum at wavelengths longer than 3500Å.

2. Spectral distribution of energy reflected by the earth's surface at wavelengths longer than 3500Å in the ultraviolet and visible regions of the spectrum.

C. Lunar orbit

1. Spectral distribution of stimulated luminescence emitted from the lunar surface in the ultraviolet and visible regions of the spectrum.

2. Spectral distribution of ultraviolet energy reflected by the lunar surface.

INSTRUMENT COMPONENTS AND FUNCTIONS

The ultraviolet instrumentation for the aircraft program includes an optical-mechanical scanning system (fig. 4) equipped with an ultraviolet sensitive photomultiple detector. Imagery produced is the line scan type. It is planned to include an emission spectrometer (fig. 9) for use in the aircraft; the spectrometer under consideration will be designed to observe one or more Fraunhofer lines in the near ultraviolet or visible part of the spectrum in earth-reflected and solar pointings.

In both earth and lunar orbital programs, the instrument package will include a) an image dissector scanning spectrometer system, and b) an integrating electronic scan imaging system, (fig. 5, Table III). Energy reflected or emitted from the earth or lunar surface will be collected by a suitable optical system (all reflective in lunar orbit), and routed by means of beam splitters to both the imaging system and the spectrometer, thus permitting recording in both spectrometer and imaging modes simultaneously. Both systems will use the same window in the spacecraft.

An essential function of the UV package in earth orbit will be to provide an engineering checkout of the integrated system in preparation for scheduled lunar orbital flights. In so achieving this function, it is expected that data will be collected pertinent 1) to detection of luminescing features on the earth's surface from orbital altitudes, and 2) to evaluation of significance of these data to the discrimination and/or identification of surface materials.

A. Aircraft program

1. Spectrometer - Primary purpose of this part of the program is to discriminate between reflected and emitted energy by means of the "line-depth technique" and a mechanically scanning spectrometer operated from aircraft altitudes. Luminescence in the spectrometer field of view will be indicated where the central intensity of the normalized Fraunhofer line spectrum reflected from the earth's surface is increased relative to central intensity of the same line observed in the solar spectrum directly. The spectrometer to be used in the aircraft program will be designed to observe at least one Fraunhofer line in the near ultraviolet or visible region of the spectrum.

2. Imager - This part of the program is already operational and is designed to produce ultraviolet imagery for identification and direct comparison of the same features imaged by other sensors operating at longer wavelengths. The instrumentation consists of an AN/AAS-5 optical-mechanical line scanner mounted in NASA's multi-sensor equipped aircraft, a Convair 240 based in Houston (fig. 4). Ultraviolet energy, reflected by ground features, falls upon a rotating mirror (A), is reflected through a light-gathering optical system (B), and focused on an ultraviolet-sensitive photomultiplier (C). The photomultiplier

output is proportional to the intensity of the ultraviolet energy incident on the photocathode. The output signal is amplified (D) and recorded on photographic film by means of the glow tube (E) whose line-scan motion is synchronized with the rotating mirror. Lateral coverage is obtained by the rotating mirror; forward coverage is obtained by the forward travel of the aircraft. The AN/AAS-5 is so-called "dual channel" scanner; thus, two detectors or photomultipliers equipped with appropriate filters may be used to view simultaneously, two selected bands in the ultraviolet, or infrared regions of the spectrum.

B. Earth orbit

1. Spectrometer - System will measure the intensity of emitted and reflected energy as a function of wavelength in selected parts of the UV and visible spectrum where prominent Fraunhofer lines are present. Luminescence in the field of view will be indicated where the central intensity of the normalized Fraunhofer line spectrum reflected from the earth's surface is increased relative to the central intensity of the same line in the solar spectrum. In order to achieve spectral resolution adequate to resolve Fraunhofer lines, it will be necessary to limit the spectral range of each image dissector to 100Å or less. Thus, five detectors (sharing the same fore optics) will be required in order to provide adequate spectral coverage (fig. 5). For example, one detector with a spectral range limited to 100Å could be used in the near ultraviolet and violet to record the K and H lines of calcium. Another detector used in the blue region could be designed to include the F line of hydrogen. These and other appropriate Fraunhofer lines are shown in Table II. Of importance is the spectral reflectance data that will be acquired in the normal course of scanning the Fraunhofer lines. These data will provide detail regarding the spectral reflectance characteristics of the earth's surface, which in some cases may be related to natural materials; i.e., rocks or groups of rocks or rock-forming minerals (fig. 3). Also, these spectral data will supplement data obtained by other methods, for example, the multispectral photography experiment.

2. Imaging - System will provide spatial information necessary for a) identification of the area integrated by the spectrometer, and b) identification of brightest features within this area. In areas where luminescence is indicated by the spectrometer, brightest features may be indicative of luminescence. Because of atmospheric attenuation factors in earth orbit, spectral range of the imaging system in the ultraviolet will be limited to the spectral band between 3500Å and 4000Å.

C. Lunar orbit

1. Reflectance

a. Spectrometry - System will provide a spectral scan whereby the intensity of emitted and reflected energy from the lunar surface will be measured as a function of wavelength. Pass band will extend from 1500Å or shorter to 3000Å. The spectrometer will provide spectral detail as to the distribution of reflected solar energy, thus supplementing spectral reflectance detail recorded by the comparatively broad band UV imaging system.

b. Imaging - System will provide imaging capability in one or more bands between 1500Å or shorter and 3000Å. This region includes that part of the ultraviolet spectrum where image contrast between rocks and common rock-forming minerals exceeds image contrast (fig. 3) at longer wavelengths.

2. Luminescence

a. Spectrometer - System will provide a spectral scan whereby intensity of emitted and reflected energy will be measured as a function of wavelength. System will be the same multi-detector spectrometer and line depth techniques described above for use in earth orbit.

b. Imaging - The imaging system described above for detection or reflected ultraviolet energy will share the same field of view with the emission spectrometer; thus, the imaging function will provide spatial information necessary for identifying the area integrated by the emission spectrometer.

METHODS FOR DATA REDUCTION AND ANALYSIS

Data reduction and analysis will include the following approached:

A. Spectral data

1. Statistical analysis of the distribution of spectral reflectance and emission; correlation of data (either by visual inspection or by means of a computer) with laboratory and field spectral measurements of known natural materials.

2. Direct comparison and correlation of spectral data with information obtained by other remote sensors.

B. Imagery

1. Precision measurement of imagery tonal values by means of a microdensitometer.

2. Compensation or normalization of image density as it varies with illumination and solar aspect angle (computer programmed)

3. Image enhancement procedures to reduce the effects of atmospheric haze (earth orbit) and to increase image contrast in selected areas.

4. Analysis of ultraviolet imagery by photointerpretive or image interpretation techniques.

5. Direct comparison and correlation of spectral data with information obtained by other remote sensors.

CURRENT SUPPORTING RESEARCH (continuing)

A. Laboratory studies

Spectral reflectance analyses have been completed on more than 50 selected rocks and rock-forming minerals in the spectral region between 2200Å and 7000Å (Watts, 1966). These studies showed that spectral reflectance of some specimens varied from more than 40 per cent in the visible to less than four per cent at some wavelengths shorter than 3000Å in the ultraviolet (fig. 3). The study also showed that although more energy is absorbed by natural material in the ultraviolet than in the visible, the highest ratios of reflected energy between most of the specimens occurs at 2500Å in the ultraviolet. Thus, a passive ultraviolet imaging system designed to operate at this wavelength in lunar orbit would permit imaging of some natural features with greater contrast than would be possible at longer wavelengths. This and other programs (Dupee, 1965) suggest that the vacuum ultraviolet region (1500Å - 2200Å) may yield spectra with more reflectance and emission spectral character or structure than has been shown at longer wavelengths. Accordingly, a program has been started to study the reflection and emission spectra of a selected group of rock and mineral samples in the vacuum ultraviolet.

B. Aircraft program

Ultraviolet imagery - Ultraviolet imagery in the 3000Å - 4000Å region is being obtained with the AN/AAS-5 optical mechanical line-scanner which is mounted in NASA's multi-sensored aircraft, based in Houston. Several flights have been conducted over several of the documented test sites, and satisfactory imagery has been obtained of several of the sites, notably Lavic Dry Lake, California (fig. 6), Meteor Crater, Arizona (fig. 7), and the sedimentary test site near Mesquite, Nevada (fig. 8). Most of these flights were conducted at an altitude of less than

5000 feet above the terrain. Recently, however, satisfactory ultraviolet imagery was obtained of the Salton Sea area from an altitude of 15,000 feet (fig. 2).

The imaging system was recently modified to permit increased sensitivity in the near ultraviolet and to permit simultaneous imaging at longer wavelengths in the visible region for the purpose of direct comparison of imagery from both regions. Laboratory measurement of variations in image density are being conducted by means of a Joyce-Loebl recording mircodensitometer and isodensitracer. These data are being used as a basis for comparison of successive sets of imagery of the same area under varying solar illumination conditions, as well as a comparison of the ultraviolet imagery with imagery obtained by other sensors operating at longer wavelengths. Signal processing and image enhancement techniques are now planned to increase contrast and reduce the effects of atmospheric scattering, particularly objectionable on ultraviolet imagery obtained from higher altitude

C. Preliminary design of orbital hardware

Studies have been completed on the evaluation of constructional and performance parameters of spectrometers and imaging systems potentially suitable for operation at orbital altitudes (Betz, 1966).

The relative merits of both interferometric and dispersive spectrometers have been considered with a view to providing a system with:

a) Spectral resolution sufficient to scan a number of selected Fraunhofer lines.

b) Spectral range sufficient to determine the reflection spectrum.

c) Sensitivity sufficient to detect luminescence of a few percent.

d) High ruggedness, with a minimum of mechanical moving parts.

A similar design study has been conducted on candidate imaging systems in an attempt to arrive at an integrated experiment package which places the minimum demands on the spacecraft in terms of window area, astronaut time, power requirements, etc., without compromising the experimental objectives. Preliminary designs from these studies appear in a later section of this document.

PROPOSED SUPPORTING RESEARCH

A. Laboratory studies

1. Reflection and emission spectra of selected rocks and rock-forming minerals in the vacuum ultraviolet, including simulation of the relatively high energy Lyman a line in the solar spectrum at 1216Å as an excitation wavelength.

2. Emission spectra of selected rocks and rock-forming minerals subjected to proton bombardment at intensities comparable to the solar flux.

B. Aircraft program

Detection by means of the line depth technique of emission spectra of natural materials produced by the solar ultraviolet at wavelengths longer than 3500Å. Preliminary feasibility study will include ground checks of potentially suitable areas in order to determine whether exposure and areal extent of luminescent materials is adequate to be detected from aircraft altitudes. Initial airborne feasibility study to follow will be conducted with a convetional off-the-shelf spectrometer similar to that shown in figure 9; spectral range will be limited to only one or two Fraunhofer lines, but spectral resolution will exceed 1Å, adequate to resolve the profile of the central intensity. Suitable areas for these tests might include salt crusts, borates, and other evaporite playa materials of alkalai and bitter lakes, such as Searles, Owens, and Borax Lakes in southern California.

C. Data reduction, correlation and interpretation

Both imaging and spectrometer sections of the experiment will use the same pre-amplification and data conditioning electroniss prior to recording the input signal on tape. The quantity of data from the orbital experiment, although not prohibitively large, will be considerable, and for this reason, as well as the desire to minimize the interface with other spacecraft equipment, the experiment will use its own high density tape recording unit. The only external information required to permit subsequent successful data correlation and interpretation will be altitude, time, and solar reference spectra. The data recording system will be designed with the capability to accept spectral and ultraviolet imager data simultaneously in earth orbit and both reflectance and emission spectra as well as ultraviolet imagery in lunar orbit.

In order to achieve quantitative meaning of the earth orbital data it will be necessary to supply some ground based measurements of the atmospheric condition at a number of specific sites simultaneously with the orbital overpasses. Supporting studies currently underway will provide a definition of ground and atmospheric data requirements, which are needed to support the proposed post-flight image enhancement procedures. These procedures are designed 1) to

minimize the atmospheric scattered component in the UV imagery data, and 2) to amplify tonal contrast. It is assumed for the present that atmospheric scattering in the UV will tend to contribute a uniform gray level over the field of view and the removal of a constant gray level from the flight data will therefore be a valid technique. It is planned to examine the validity of this procedure by collecting imagery from increasing aircraft altitudes between now and the flight hardware construction phase.

Data rates and bulk weights for both earth and lunar orbits are estimated in Table III.

ORBITAL CHARACTERISTICS

A. Earth

1. Altitude: 200 km.
2. Ground speed: 7 km/sec.
3. Ground FOV: 10 km^2 (1^o optical system for spectrometer)
   300 km^2 (5^o optical system for imager)

B. Lunar

1. Altitude: 80 km.
2. Ground speed: 1.5 km/sec.
3. Ground FOV: 2 km^2 (1^o optical system for spectrometer)
   50 km^2 (5^o optical system for imager)

ENGINEERING INFORMATION [1/]

A. Earth orbit

The instrument package will include a spectrometer system with a one-degree field of view and an imaging system with a five-degree field of view. The component configuration of the package is such that both the imager and spectrometer will share the same spacecraft window, fore-optics, and data recording system; for the purposes of this proposal, however, these two systems will be discussed separately. Components of both systems are adaptions of off-the-shelf items, and hence, lead time is minimal and prototype design and construction does not require an extensive developmental program. Moreover, both the imaging and spectrometer functions are designed so that scanning is achieved electronically, thereby avoiding problems of mechanically moving parts in a launch and space environment.

1. Spectrometer - The spectrometer described herein is designed primarily for detection of Fraunhofer lines, but will, in addition, provide reflectivity data throughout parts of the ultraviolet and visible regions of the spectrum immediately adjacent to each Fraunhofer line (fig. 1).

   a. Description of components - The equipment is to consist of an electronically scanned grating spectrometer of 0.5Å resolving power, resolution that is required to adequately detect the central intensity of selected Fraunhofer lines.

      To achieve a spectral resolution of 0.5Å, and to integrate a one-degree area on the ground, the spectrometer specifications shown in Table IV have been determined.

      An image dissector, such as the type #F4011 manufactured by International Telephone and Telegraph (ITT) (Appendix A), is to be used as the detector element. This device permits the spectral scan to be achieved electronically. The choice of Fraunhofer lines shown in Table II would require five image dissectors arranged in two rows as shown in figure 5. The image dissectors are arranged to scan each line and well into the wings. Thus, the five image dissectors will provide a spectral scan from which the broad spectral curve of the luminescence can be determined. In addition, spectral reflectance data will be obtained in spectral regions immediately adjacent to each Fraunhofer line.

1/ Engineering feasibility studies were conducted by IIT Research Institute, Chicago (See Betz, 1966).

In order to compare the shape of each Fraunhofer line in the reflected spectrum from the earth's surface to the same line in the solar spectrum, it is necessary to view the sun periodically with the spectrometer. This can be accomplished with a fiber optics bundle, one-quarter or three-eights inch diameter which can be extended to any convenient position on the surfac of the spacecraft exposed to sunlight.

A scattering plat or ground glass would be attached to the exposed end. The inner end will be near the entrance slit and will be periodically (perhaps every minute or two) reflected into the slit by an electrically operated mirror (fig. 5).

b. Signal-to-noise ratio - Due to the small cathode area of the image dissector, the dark current is small compared to the signal current. Therefore, one may consider that the noise of the image dissector is essentially the noise in signal and is expressed as:

$$N = \sqrt{2 e i \Delta f} \qquad (1)$$

where $\underline{i}$ is the cathode current, $\underline{\Delta f}$ is the frequency band width, and e is the charge on the electron. Writing (1) in terms of irradiance on the cathode, the equation becomes:

$$N = \sqrt{2 e H_d AS \Delta f} \qquad (1)$$

where H_d = irradiance at the detecto

A = area of detector

S = sensitivity in amp. $watt^{-1}$

The ratio of the signal to the noise in signal is:

$$S/N = \sqrt{\frac{H_d A S}{2 e \Delta f}} \qquad (2)$$

By incorporating the characteristics of the spectrometer, this can be written in terms of the ground irradiance thus:

$$S/N = \sqrt{\frac{I\Omega A\, r\tau}{2e\Delta f}} \qquad (3)$$

where I = irradiance of the earth (moon)

r = reflectance of the earth

Ω = solid angle of collection for spectrometer

τ = transmission of the entire optical system.

Substituting in Equation (3) for the irradiance in the wings of a Fraunhofer line, and similarly for the center, one may calculate the signal to noise and hence determine the precision of the measurement. Table V summarizes the calculations for two Fraunhofer lines: C (6562Å), and F (4861Å).

The angular velocity in earth orbit is 2° per second or 7 km per second at an altitude of 200 km. Therefore, it would be desirable to complete one spectral scan in 1/2 second in order to provide $1^{\circ} \times 1^{\circ}$ field of view for each spectral scan. Accordingly, a bandwidth of 100Å per scan, with a resolution of 0.5Å, will require 400 spectral elements per second. As electronic bandwidth of 600 cycles is assumed as reasonable. Signal to noise in the wings and center of both the C and F Fraunhofer lines is calculated in Table V.

These values indicate that in the C line, one can measure the central intensity to about seven percent and the continuum level to 2.5 percent. For the F line, the center can be measured to about 2.5 percent while the wings can be measured to about one percent. Should laboratory tests indicate that some of these values are marginal, the S/N ratios can be improved by reducing the spectral width from 100Å to 50Å.

2. Imaging System (integrated with the spectrometer system)

   a. Description of components - Both the spectrometer and imaging systems will share the same fore-optics. The spectrometer, with its one-degree field of view, will use the central part of the collector lens; the imaging system with its five-degree field, will use the periferal area of the same lens (fig. 5). No auxillary optics are required. Because the imaging system and spectrometer are one unit, they will require only the one window in the vehicle.

Figure 10 shows the area covered by the spectrometer and imaging system with the system fixed in the spacecraft so as to look vertically downward. A complete schematic diagram of the entire optical system is shown in figure 11.

b. Signal to noise - The useful area on the faceplate of the image dissector is about 25 mm x 25 mm. Assuming a resolution element of 125 microns, 200 elements will be required for each scan line. Using the spacecraft's forward velocity to perform the scanning function in the direction of flight, the scanning rate normal to the line of flight must be 80 lines per second in order to provide equal resolution in both directions. Assuming a gray scale of 15 levels, the electronic bandwidth for this system is about 3.2×10^4 cycles per second.

Specifications of the imaging system are shown in Table VI.

Signal to noise calculations for various spectral bandwidths are shown on Table VII.

B. Lunar orbit - The three components being considered for the ultraviolet experiment in lunar orbit are:

1. Spectrometer - to measure spectral distribution of luminescence in the ultraviolet and visible regions emitted by parts of the lunar surface.

2. Spectrometer - to measure spectral reflectance of the lunar surface in the ultraviolet ($<$1500Å-4000Å).

3. Imaging - to measure the lunar surface in one or more ultraviolet bands ($<$1500Å-3000Å).

Signal to noise calculations are summarized in Table VIII.

1. Emission spectrometer - Equipment for this study will be the same as that tested in earth orbit.

2. Reflectance spectrometer - Instrument package will include an image dissector used as the detector element on a grating spectrometer of the Ebert type. Resolving power would be on the order of 10Å; field of view would be one degree. The image dissector would feature an S-20 photo cathode and lithium fluoride or sapphire window, thus extending sensitivity to wavelengths shorter than 2000Å. Specifications of the ultraviolet reflectance spectrometer are shown in Table VIII and signal to noise ratios in Table IX.

3. Imaging - System would employ an image dissector type imaging system similar to that described for earth orbit, except that system would be capable of operating in one or more bands in

the ultraviolet including wavelengths as short or shorter than 1500Å. Imaging system would be integrated with reflectance spectrometer system into a single package. Both systems would use the same fore-optics -- the spectrometer with its one-degree field of view would use the central part of the collector lens; the imaging system with its five-degree field of view would use the periferal area of the same lens.

REFERENCES

Betz, Howard, 1966, Comparative study of ultraviolet instrumentation suitable for orbital remote sensing experiments: IITRI Tech. Rept. prepared for U.S. Geol. Survey under Contract No. 14-08-0001-10360, Technical Letter NASA-31.

British Sulphur Corp., Ltd., 1961, World survey of phosphate deposits: British Sulphur Corp., Ltd., London, v. III, p. 11.

Dubois, Jr., (in Kopal) 1962, The luminescence of the lunar surface: Physics and Astronomy of the Moon, Academic Press, New York, p. 392-394.

Dupee, W.D., 1965, The response of selected rock specimens to vacuum ultraviolet light, (unpub. thesis): Air Force Institute of Tech., Air University, Wright-Patterson Air Force Base, Ohio, 135 p., 46 illus.

Fischer, W.A., and Gerharz, R., 1964, Measurement of ultraviolet reflectance, (unpub.): U.S. Geological Survey Technical Letter NASA-3.

Foster, W.R., 1948, Useful aspects of the fluorescence of accessory mineral zircon: Amer. Mineralogist, v. 32, no. 11-12, p. 724-735.

Gleason, Sterling, 1960, Ultraviolet guide to minerals: D. Van Nostrand Co., New York, 244 p.

Greenman, N.N., and others, 1965, feasibility study of the ultraviolet spectral analysis of the lunar surface: Douglas Aircraft Co. rept. prepared under NASA Contract NAS9-3152.

Hemphill, W.R., and Gawarecki, S.J., 1964, Ultraviolet video imaging system, (unpub.): U.S. Geol. Survey Tech. Letter NASA-3.

Hemphill, W.R., Fischer, W.A., Dornbach, J.E., 1965, Ultraviolet investigations for lunar missions: Proc. 11th Ann. Meeting Amer. Astronautical Soc., May 4-6, Chicago, Illinois.

Kopal, Z., 1965, The luminescence of the moon: Scientific American, v. 212, no. 5, p. 28-37.

Kozyrev, K.A., (in Kopal) 1962, The luminescence of the lunar surface: Physics and astronomy of the moon, Acad. Press, New York, p. 392-394.

Lipson, H., Nov. 1965, Lunar luminescence: Inst. Physics and the Physical Sci. Bull., v. 16, no. 11, Univ. of Manchester, Manchester, England.

Luckiesh, 1946, Applications of germicidal, erthymal, and infrare energy: D. Van Nostrand Co., New York, p. 383.

Mimmaert, C.F., Mulders, W., and Hootgast, J., 1940, Photometric atlas of the solar spectrum: Univ. of Utrecht, Utrecht, Netherlands.

Myronova, M.M., 1965, Luminescence in the crater Aristarchus (Abst.): Main Astron. Observatory, Acad. Sci. of the Ukranian Soviet Socialist Repub., Kiev, Dopovidi, AN Ukr. RSR, no. 4.

Nash, D.B., 1965, Proton-excited silicate luminescence: experimental results and lunar implications: presented in part at the 46th Ann. Meeting AGU, Washington, D.C., April 19-22, 1963. To be published in the Jour. Geophys. Research.

Riecker, R.E., 1962, Hydrocarbon fluorescence and migration of petroleum: Bull. Amer. Assoc. Petroleum Geologists, v. 46, no. 1, p. 60-75.

Spinrad, H., 1964, Lunar luminescence in the near ultraviolet: Icarus, v. 3, p. 500-501.

Watts, H., 1966, Laboratory measurement of ultraviolet reflection (2200-7000Å) and stimulated emission of rocks and rock-forming minerals: IITRI Tech. rept. prepared for the U.S. Geol. Survey under Contract No. 14-08-0001-10360, Technical Letter NASA-32

Figure 1 a. Line-depth profiles of the K and H lines of calcium (3934Å and 3968Å, respectively) in the solar spectrum reflected from the lunar surface. The central depth of both lines in the lunar spectrum is shallower than the same lines observed in the solar spectrum directly, thus indicating that a luminescing area was included in the spectrometer field of view. (Profile was recorded by Hyron Spinrad, University of California, Berkeley; reprinted in Kopal, 1965).

b. Profile of the C line of hydrogen (Minnaert, et al, 1940).

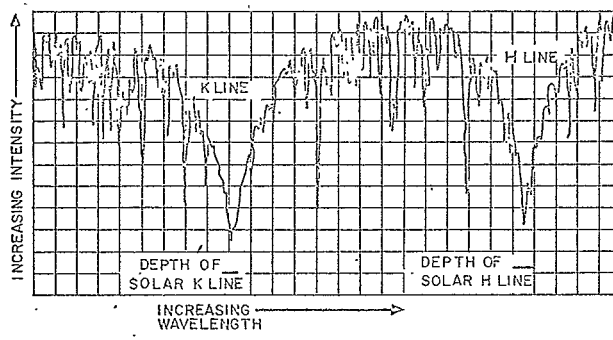

PROFILE OF CALCIUM H AND K LINES
(From Spinrad)

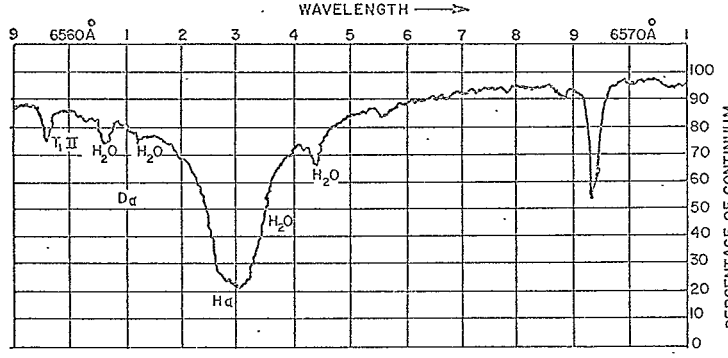

PROFILE OF HYDROGEN C LINE
(Taken from the Utrecht Atlas)

IITRI/ASC

Figure 1

Figure 2. Ultraviolet line-scan imagery of the Salton Sea area taken from an altitude of 15,000 feet. 1/ Gray scale shows marked contrast between cultivated fields. Red Island, composed of rhyolite obsidian is shown at a; Mellet Island b; c indicates a tonal variation which may be caused by a turbidity current where the Alamo River, d, empties into the sea. Areas that are highly reflective in the ultraviolet are shown at e and at f on the northern tip of Red Island. Specific material causing this high reflectivity is not known.

1/ See classified (confidential) supplement number 33A.

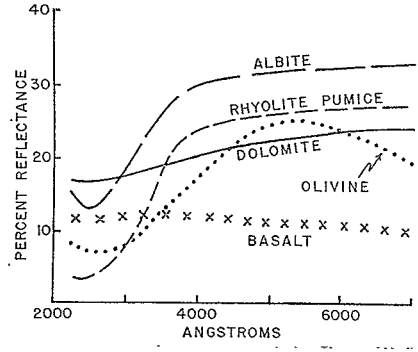

Figure 3

Reflectance spectra of some common rocks and rock-forming minerals.

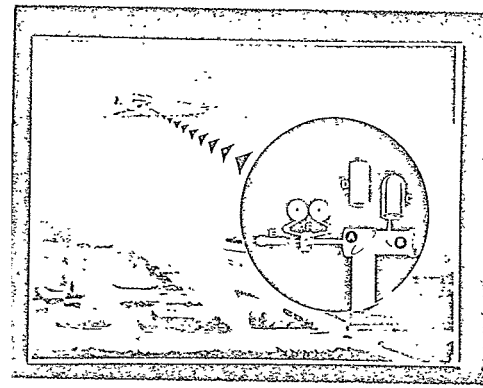

Figure 4

Ultraviolet line-scan imaging system. Operational components include a rotating mirror, A; collecting optics, B; photomultiplier, C; amplifier, D; glow-tube, E; and photographic recorder, F. (Modified from diagram supplied by the HRB-Singer Corporation.)

Figure 5 Sketch showing both imaging and spectrometry systems integrated into one instrument package.

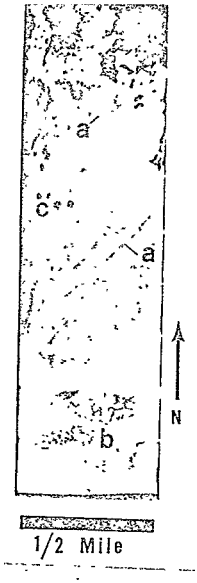

Figure 6

Line-scan imagery of part of Lavic Dry Lake, San Bernardino County, California. Flight altitude was 2000 feet above the terrain. The photomultiplier used to detect reflected ultraviolet energy employs a 6362 glass envelope tube and an S-11 spectral response. Roads may be seen at a; cracks due to drying of the lake bottom may be seen at b; dark-toned spots at c are bomb craters.

Figure 7. Ultraviolet line-scan imagery of Meteor Crater, taken from a flight altitude of 4500 feet. 1/ Dark line on imagery below rim marks break in slope between bedrock areas above, and unconsolidated detrital material below. Light toned areas, indicated by a, are outcrops of a light red sandstone near the base of Moenkopi Formation of Triassic age. Contrast between this sandstone and the underlying Kiabab Limestone of Permian age is more pronounced on the UV imagery than conventional air photographs taken simultaneously. Other highly reflective materials include the unconsolidated alluvium in dry stream washes, b, as well as debris around the margin of the crater, c, and within the rim, d. Talings from exploratory shafts appear at e. Abrupt tonal contrasts along scan lines in vicinity of crater, may be due to operator manipulation of controls during overflight.

1/See classified (confidential) supplement number 33A.

Figure 8. Ultraviolet line-scan imagery of NASA's remote sensor sedimentary test site near Mesquite, Nevada. 1/ Imagery was taken from an altitude of 3500 feet above the terrain. Image contrast between alternating bands of basalt and underlying alluvial deposits of Tertiary age is greater on the ultraviolet imagery than on conventional air photographs taken simultaneously.

1/See classified (confidential) supplement number 33A

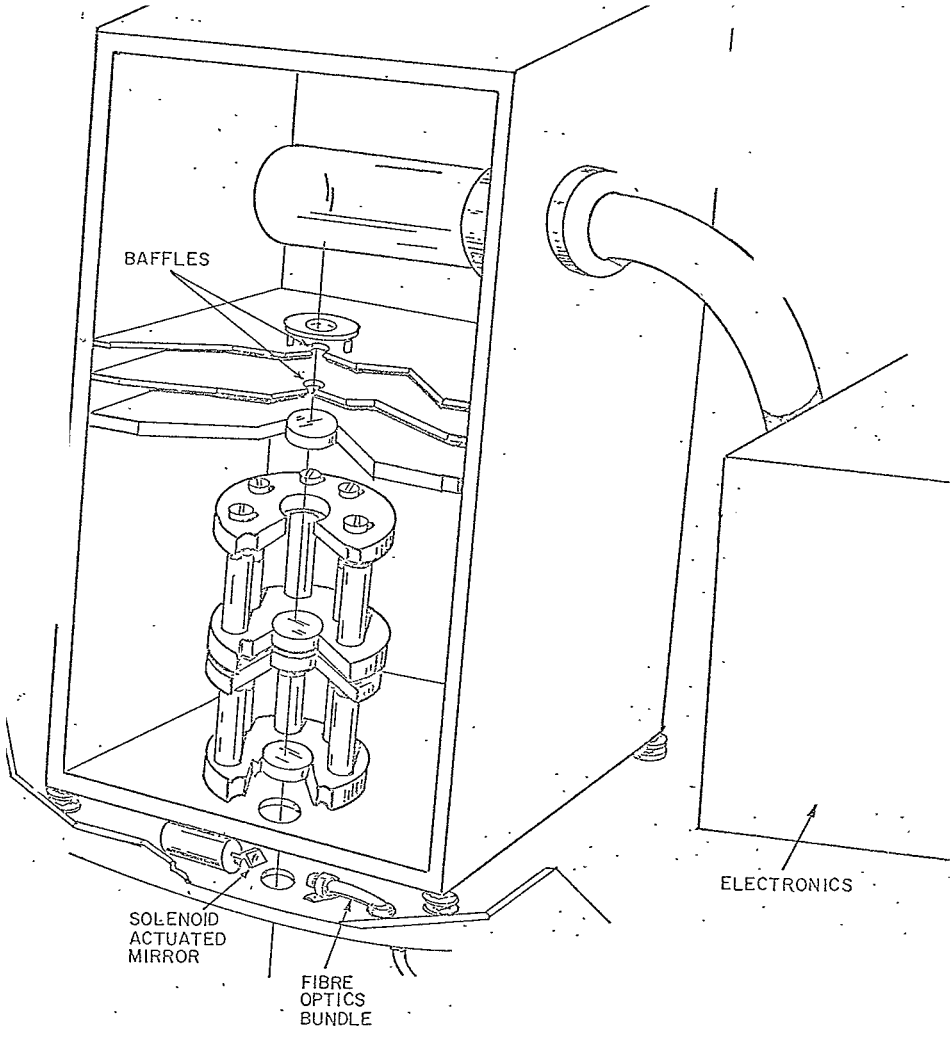

NTERFEROMETER FOR LUMINESCENCE DETECTION FROM AIRCRAFT ALTITUDES

Figure 9

TRI/ASC

Sketch showing interferometer-spectrometer for detection of luminescence from aircraft altitudes.

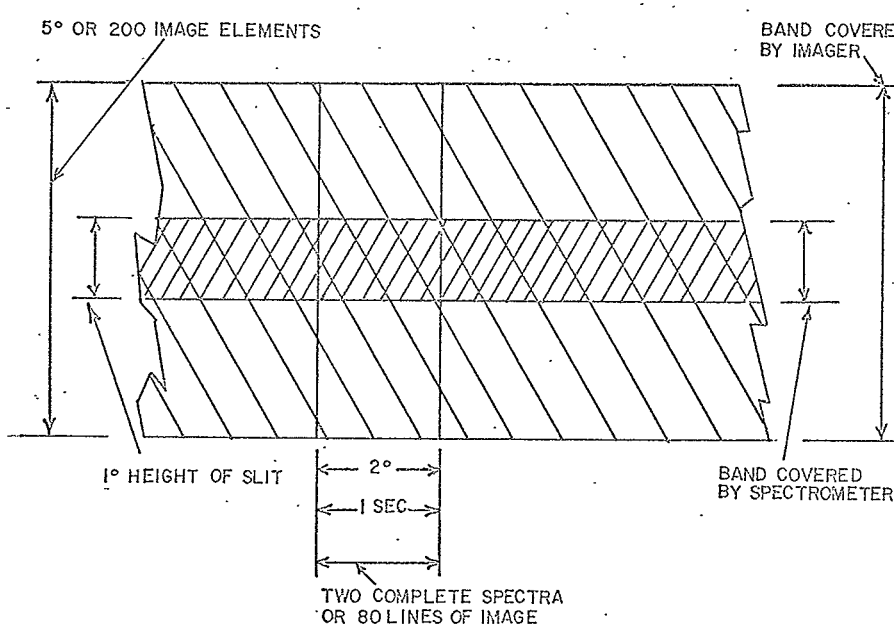

Figure 10 AREA VIEWED BY SPECTROMETER AND IMAGING SYSTEM

Ground plot of area viewed by combined spectrometer imaging system in earth orbit.

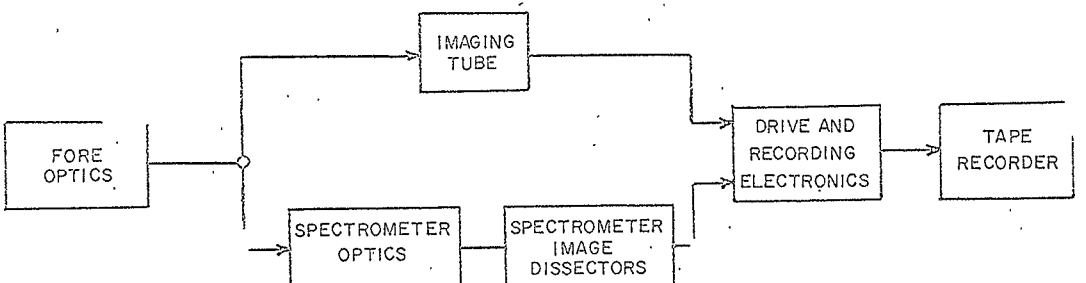

Figure 11

Block diagram showing electronic and optical components of the integrated spectrometer-imaging system.

TABLE I

Luminescent intensities in specific lunar regions
after Dubois (in Kopal, 1962)

Lunar Region Observed	Values for luminescence for different colors: Red 6563	Yellow 5893	Green 5200	Blue 4861	Violet 4300
Southwest Limb Lat. 45°S		0.14	0.20	0.04	
Region between the Maria Serenitatis and Pluvium (Lat. 30°N, Long. 8°W)		0.05			0.06
Center of Sinus Medii	0.12			0.10	
Mare Tranquilitatis (Lat. 0°, Long. 28°W)		0.14			
Mare Foecunditatis (Lat. 0°, Long. 50°W)	0.08	0.10		?	
Floor of crater Regiomontanus	0.25	0.13		0.05	
Mare Crisium		0.15	0.20	0.08	
Mare Frigoris (Western Region)		0.06	0.07	?	0.04
Region around Lat. 12°S, Long. 60°W		0.10			0.03
Mare Vaporum	0.12	0.07		0.14	
Oceanus Procellarum (Central and Southwestern region)	0.20				0.10

TABLE II

Fraunhofer lines in the near ultraviolet and visible regions of the spectrum, suitable for observation by the line depth method.

Line	Color	Wavelength	Source
C	red-orange	6563Å	Hydrogen
D_1	yellow	5896Å	Sodium
D_2	yellow	5890Å	Sodium
F	blue	4861Å	Hydrogen
G	Violet	4340Å	Hydrogen
H	deep violet	3968Å	Calcium
K	deep violet	3934Å	Calcium

Table III

PERFORMANCE FACTORS OF INSTRUMENTS DESIGNED TO MEASURE ULTRA
AND LUMINESCENCE OF THE EARTH AND LUNAR SURFACE MATERIALS FROM

	Instrument	Objective	Spectral Range (tent.)	FOV	Spat. Res.	Spec. Res.	Type of Coverage	Prospect Users
Aircraft	1. Emission spectrometer (conventional mechanically scanning type)	Detection of luminescing features in FOV	Limited	5°	NA	< 1Å	Non-imaging	Geologists geographe oceanogra agricultu etc.
	2. Imaging system (AN/AAS-5 optical-mechanical line scanner)	a. Identification of spectrometer pointings. b. Spatial identification of surface features with high reflective coefficients	< 3500Å-4000Å	< 90°*	< 4mr	NA	Imaging	
Earth Orbit	1. Emission spectrometer image dissector (electronic scan)**	Detection of luminescing features in FOV***	3900Å-6700Å (intermittent)	1°	NA	< 1Å	Non-imaging	Geologists geographe agricultu oceanogra etc.
	2. Imaging system (image dissector electronic scan)**	a. Identification of spectrometer pointings. b. Spatial identification of surface features w high reflective coefficients in the UV	< 3500Å-4000Å	5°	< 20m	NA	Imaging	
Lunar Orbit	1. Emission spectrometer (image dissector electronic scan)**	Detection of luminescing features in FOV	< 3900Å-6700Å (intermittent)	1°	NA	1Å	Non-imaging	Geologist lunar sci
	2. Reflection spectrometer (image dissector electronic scan)**	Spectral reflectance detail	< 1500Å-> 8000Å	1°	NA	20Å	Non-imaging	
	3. Imaging system (image dissector electronic scan)**	a. Imagery in one or more bands simultaneously. b. Identification of spectrometer pointings	< 1500Å-3000Å	5°	< 20m	NA	Imaging	

* Line-scanner FOV is normal to the direction of flight.
** All instruments, both imaging and non-imaging will be integrated into one instrument package. An all-reflective optical system will be used for the lunar orbital package.
*** A reflection spectrum will also be obtained in the normal course of obtaining the spectral sc

OLET REFLECTION

RBITAL ALTITUDES

ve	Data Rate	Weight (lb)	Vol. (ft^3)	Tape Recorder Wt/Vol	Total Power (watts)	Total Data Bulk (lbs) (including tape reels)	
, ers, sts,	1.5 kbs/ sec	150	3	?	< 50		
	100 kbs/ sec	200	5	NA	< 75		
; , sts, ers,	10 kbs/ sec	< 100 (6 image dissectors 30 lb; optics-40 lb; electronics-20 lb)	2	< 30 lbs/ < 1 ft^3	< 50	22 lb	for 20% surface coverage and 3 x 10^4 bits/$inch^2$ tape packing density.
	100 kbs/ sec	Integrated with spectrometer				145 lb	
and tists	10 kbs/ sec	< 150	< 3	< 40 lb/ < 1.5 ft^3	< 75	7.5 lb	
	10 kbs/ sec	Integrated with emission spectrometer and imaging system				5 lb	for 14 day missions 16% coverage is possible with a 5° F.O.V. from 80 km.
	> 100 kbs/ sec	Integrated with emission and reflection spectrometer				125 lb	

d will share the same fore-optics.

for emission.

TABLE III

TABLE IV .

Specifications --- earth orbital emission spectrometer (Czerny-Turner type).

Grating size	100 x 100 mm
Grating spacing	1200 lines/mm
Focal length of colimator	50 cm
Effective aperture	F/4.5
Dispersion (1st order)	17A/mm
Slit size	0.51 cm by 2.5×10^{-3} cm
Slit area	1.3×10^{-3} cm^2
Resolution (with above slit)	0.4A at 5000A
Scan range	425A

TABLE V

Signal-to-noise ratios of the C and F Fraunhofer lines, including both the center and the continuum immediately adjacent to the line.

$$S/N(C,\ 6562\text{Å},\ \text{center}) = \frac{3.6 \times 10^2}{\sqrt{600}} = 14.5$$

$$S/N(C,\ 6562\text{Å},\ \text{continuum}) = \frac{9.2 \times 10^2}{\sqrt{600}} = 38$$

$$S/N(F,\ 4861\text{Å},\ \text{center}) = \frac{9 \times 10^2}{\sqrt{600}} = 37$$

$$S/N(F,\ 4861\text{Å},\ \text{continuum}) = \frac{2.3 \times 10^3}{\sqrt{600}} = 94$$

TABLE VI

Specifications —— earth orbital imaging system

Cathode		S-20
Scan area		2.5 cm x 2.5 cm 1 inch x 1 inch
Scan element		.0126 cm x .0126 cm (.001 in. x .001 in.)
Area of scan element	=A=	1.6×10^{-4} cm^2
Optical collector		F/2.5 photographic objective
Solid angle of collector	=	8.6×10^{-2} ster

(This is the peripheral area when square area for spectrometer is removed)

Transmission of objective estimated at - 0.60

TABLE VII

Signal-to-noise --- earth orbital imaging system 1/

Spectral Band	N* Irradiance of earth at sea level watt cm^{-2}	H Radiance of earth (20% reflectivity) watt cm^{-2} $ster^{-1}$	S Average over the wavelength interval amp $watt^{-1}$	S/N ($4f = 3.2 \times 10^4$
3600Å to 4200Å	26×10^{-4}	1.7×10^{-4}	5×10^{-2}	82
3600Å to 4000Å	14×10^{-4}	0.88×10^{-4}	5×10^{-2}	58

1/ Assuming:

r = 0.6 - transmission of the optical system

r = 20% - reflectivity of the earth surface

$\Delta f = 3.2 \times 10^4$

* See Ref. 5 for radiance values.

TABLE VIII

Specifications - lunar orbital reflectance spectrometer

Effective aperture	F/4.5
Focal length of collimator	5 inches (13 cm)
Reciprocal linear dispersion	131 Å/mm
Spectral range (one grating position)	3000 Å
Resolution ($\Delta\lambda$)	10 A
Spectral responses of cathode (sapphire or LiF window)	S-20
Grating	600 lines/mm
Slit dimensions	0.002"x 0.2"
Scan rate	1 or 10 spectra/sec
Power required	20 watts
Weight	25 lbs.

TABLE IX

Signal-to-noise --- lunar orbital reflectance spectrometer

Wavelength in Å	Irradiance of Lunar Surface Watts Cm^{-2} $Å^{-1}$	Radiance of Lunar Surface Reflectivity 0.1 Watts Cm^{-2} $Å^{-1}$ $ster^{-1}$	Sensitivity of Detector Amps/watt (S-20 photocathode with a sapphire window)	S/N	S/N 1 scan/sec 250 elements/sec
1500	1×10^{-8}	3.2×10^{-10}	2.2×10^{-2}	$\frac{7.3 \times 10^{1}}{\sqrt{\Delta f}}$	6.5
2000	14×10^{-6}	4.5×10^{-8}	3×10^{-2}	$\frac{1.1 \times 10^{3}}{\sqrt{\Delta f}}$	9.8×10^{1}
3000	5×10^{-6}	1.6×10^{-7}	4×10^{-2}	$\frac{2.2 \times 10^{3}}{\sqrt{\Delta f}}$	2×10^{2}
3500	12×10^{-6}	3.8×10^{-7}	4.5×10^{-2}	$\frac{3.5 \times 10^{3}}{\sqrt{\Delta f}}$	3.1×10^{2}
4000	11×10^{-6}	3.5×10^{-7}	5×10^{-2}	$\frac{2.3 \times 10^{3}}{\sqrt{\Delta f}}$	2×10^{2}

Reflectivity of lunar surface assumed to be 10%
Scan is 2500Å or 250 spectral elements/scan
Transmission of entire optical system including grating is 10%

APPENDIX A

ENTATIVE DATA

MAGE DISSECTOR

Type F4011

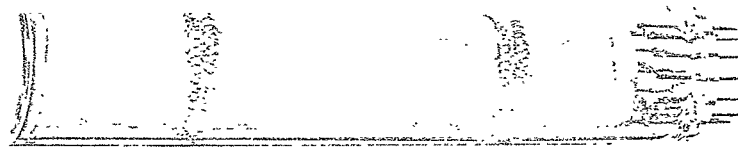

The F4011 model number designates a family of 1-1/2 inch diameter magnetically focused and deflected image dissector camera tubes. Image dissectors in this series can be provided with S-1, S-11, and S-20 type photocathodes, and with various scanning aperture shapes and sizes ranging from approximately 0.0005 inch to 0.35 inch (Notes 1 and 3).

The image dissector has several properties which make it well suited to such applications as slide-projector readers, hard-copy readers, electronically scanned spectrometers, flaw detectors for industrial process controls, and electronic star trackers. A few of these image dissector properties which should be considered when selecting an appropriate camera tube for a specific application are: (a) high resolution-determined primarily by the size of the defining aperture (b) nonstorage - allowing the scan rate to be varied without changing the signal current amplitude (c) reliable operation over a long period of time - simple rugged construction and lack of thermionic cathode and (d) linear dynamic range of several orders of magnitude.

GENERAL CHARACTERISTICS

Photocathode spectral response (Note 1)	S-1, S-11, or S-20 (See Figure 1)
Focusing method (Note 2)	Magnetic
Deflection method (Note 2)	Magnetic
Aperture size limits (Notes 1 and 3)	0.0005 to 0.350 inch
Number of dynodes (Note 4)	10

MECHANICAL CHARACTERISTICS

Window material	Corning 7056 or equivalent
Window index of refraction	1.5
Window thickness	0.080 ± 0.005 inch
Maximum useful photocathode diameter	1.1 inches
Maximum tube diameter	1.5 inches
Maximum over-all tube length	8.2 inches
Weight (approximate)	5.5 ounces
Base	Small button, 14 pin
Mounting position	Any

RECOMMENDED OPERATING CONDITIONS

Photocathode voltage	-2400 volts
Drift tube and dynode No. 1 voltage	-1800 volts
Dynode No. 2 voltage	-1645 volts
Dynode No. 3 voltage	-1490 volts
Dynode No. 4 voltage	-1335 volts
Dynode No. 5 voltage	-1180 volts
Dynode No. 6 voltage	-1025 volts
Dynode No. 7 voltage	-870 volts
Dynode No. 8 voltage	-715 volts
Dynode No. 9 voltage	-560 volts
Dynode No. 10 voltage	-325 volts
Anode voltage	0 volts
Ambient temperature	25° C
Nominal axial magnetic field strength with 600 volts between photocathode and drift tube/dynode No. 1 (Note 5)	40 gauss

TENTATIVE PERFORMANCE CHARACTERISTICS

For recommended operating conditions:

	Minimum	Typical	
Cathode luminous sensitivity (Notes 6 and 7)			
S-1	12	20	μa/lumen
S-11	30	40	μa/lumen
S-20	80	100	μa/lumen
Cathode peak radiant sensitivity (Note 7)			
S-1 (8000 Å)	--	0.0022	amperes/watt
S-11 (4400 Å)	--	0.032	amperes/watt
S-20 (4200 Å)	--	0.043	amperes/watt
Current amplification	5×10^4	5×10^5	
Typical paraxial resolution (Note 8)	--	1500	tv lines/inch
Typical off-axis resolution, static focus (Note 9)	--	800	tv lines/inch
Typical off-axis resolution, dynamic focus (Note 9)	--	1200	tv lines/inch
Image distortion	See Note 10		
Deflection linearity	See Note 11		

MAXIMUM RATINGS

Absolute Maximum Values

Average photocathode current density (Note 12)	10 μa/cm^2
Average anode current (Note 12)	100 μa
Peak anode current (Note 13)	250 μa
Ambient temperature	75° C
Over-all voltage	3400 volts
Photocathode to drift tube and dynode No. 1 voltage	1000 volts
First dynode to anode voltage	2400 volts
Dynode No. 9 to Dynode No. 10 voltage	300 volts
Last dynode to anode voltage	400 volts

NOTES

1. When ordering an F4011, two specifications in addition to the series designation "F4011" are required, namely: (1) the type of spectral response desired, and (2) the dimension of the defining aperture in mils. These two numerical specifications should follow the series designation in brackets as follows:

EXAMPLE 1: AN F4011 (S1, 2R). This calls for an F4011 image dissector with an S-1 type photocathode and a 0.002 inch diameter round defining aperture.

EXAMPLE 2: An F4011 (S-11, 1S). This calls for an F4011 image dissector with an S-11 type photocathode and a 0.001 inch x 0.001 inch square aperture.

EXAMPLE 3: An F4011 (S-20, 4 x 100). This calls for an F4011 image dissector with an S-20 photocathode and a 0.004 inch x 0.100 inch slit shaped rectangular aperture.

2. The F4011 is designed to utilize the standard deflection and focus coil assembly available commercially for 1-1/2 inch OD vidicons (such as the RCA 8051 vidicon). Custom built coils for improved resolution and reduced distortion are also available from ITTIL.

3. The F4011 is available with aperture sizes and shapes varying within the dimensional limits of 0.0005 inch and 0.35 inch. A typical aperture diameter would be 0.0015 inch. Added tooling costs may be involved if specialized sizes or shapes are required.

4. Additional dynodes can be supplied on special order.

5. All commercially available focus solenoids have a substantial variation in magnetic field intensity along the axis of the coil. For example, in the Cleveland Electronics CE1 15VFA-259 vidicon coil assembly, when the image section of the F4011 (5 inches long from photocathode to defining aperture) is centered in the focus field, the axial field strength varies by a factor of 2.5 from the extremes to the center of the drift space. By relocating the photocathode closer to the "waist" of the solenoid field, the ratio of magnetic flux density at the photocathode to flux density at the defining aperture is increased. Resultant image magnification increases resolution at the cost of S/N. This maneuver is equivalent to adjusting aperture size.

6. With 10^{-2} lumen source of 2870 degrees K color temperature (illumination normal to plane of window).

7. At 270 volts dc applied between photocathode and all other elements connected together.

8. For aperture sizes exceeding approximately 0.003 inch the resolution capabilities of the F4011 can be predicted quite accurately based on the known aperture size and shape. For example, an F4011 with a 0.010 inch square aperture will give very nearly 100 percent modulation when scanning a 100 tv lines per inch by (50 line pairs per inch, each line being 0 010 inch wide) pattern of equal light and dark bars at right angles with the square aperture aligned with the scan direction (assuming no bandwidth limitations on the response frequency) In the 0 001 inch to 0.003 inch size region and below, the absolute emission energy of the photoelectrons begins to play a significant role in the resolving power, depending on the wavelength of the input radiation, the type of photocathode, the accelerating voltage selected for the tube, etc. Figure 2 shows the measured paraxial resolution characteristics for an F4011 with a 0.001 inch round aperture under recommended operating conditions. The percentage modulation of 25 percent achieved in this tube at 1500 tv lines/inch (1000 tv lines/vertical raster height) is particularly noteworthy.

9. At 0.75 inch image diameter. The F4011 utilizes a unique new electron-optical design (patent applied for) to achieve optimum off-axis imaging properties. This new design represents a noteworthy improvement in the already excellent characteristics of the magnetic focusing - magnetic deflection combination used so successfully in image orthicon and vidicon television camera tubes, as well as in the majority of ITTIL image dissectors.

For many applications, particularly when using the F4011 with one of the larger apertures (See Note 4), off-axis resolution losses are difficult to observe experimentally. For smaller aperture tubes under limiting resolution conditions, the losses appear to be approximately as given ITTIL should be consulted for the latest information on this parameter.

Static focus applies to a fixed focus condition, adjusted for optimum paraxial focus. Some over-all improvement in average resolution can be achieved by static focusing at some intermediate radial position instead.

Dynamic focus applies to a condition in which small adjustments in the focusing magnetic field or electric field are made in synchronism with the scan in order to achieve optimum focus at the particular image area being observed. Dynamic focus is required for the ultimate in over-all resolving power.

10. Image distortion in the F4011 has not yet been determined. Because of the unique electron optical design and the well known low distortion characteristics of solenoidal magnetic focusing and deflection (e. g. 1-1/2 inch vidicon), distortion is expected to be low, probably much less than 5 percent.

11. Linearity of deflection (scan position versus deflection current) in the F4011 is expected to be similar to the 1-1/2 inch vidicon, i e. very good. Reproducibility of scan position versus deflection current is often of greater significance and is expected to be excellent provided the scan coils are not allowed to shift position with respect to the tube and various power supplies (focus, accelerating voltages, etc.) are stabilized. ITTIL should be consulted for up-to-date quantitative information on image distortion and scan linearity.

12. Averaged over any interval not greater than 1 second.

13. For 10-percent maximum departure from linearity of output current versus input flux.

14. Registered JEDEC response curve. All spectral responses are normalized to 100 percent following registered JEDEC recommendations. Permissible tolerances on these various registered S-response curves have been or are being established by JEDEC.

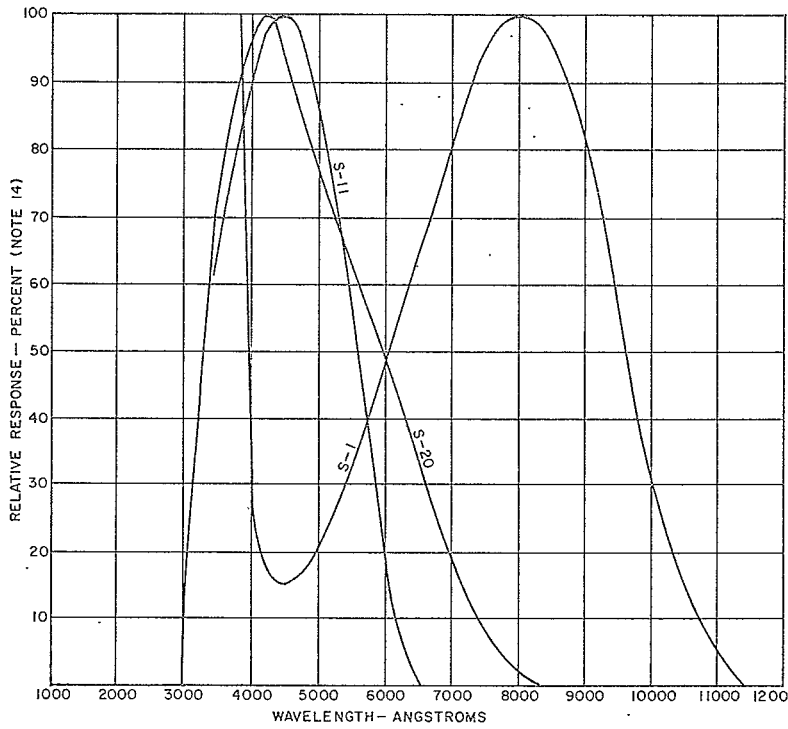

Figure 1 Spectral-Sensitivity Curves

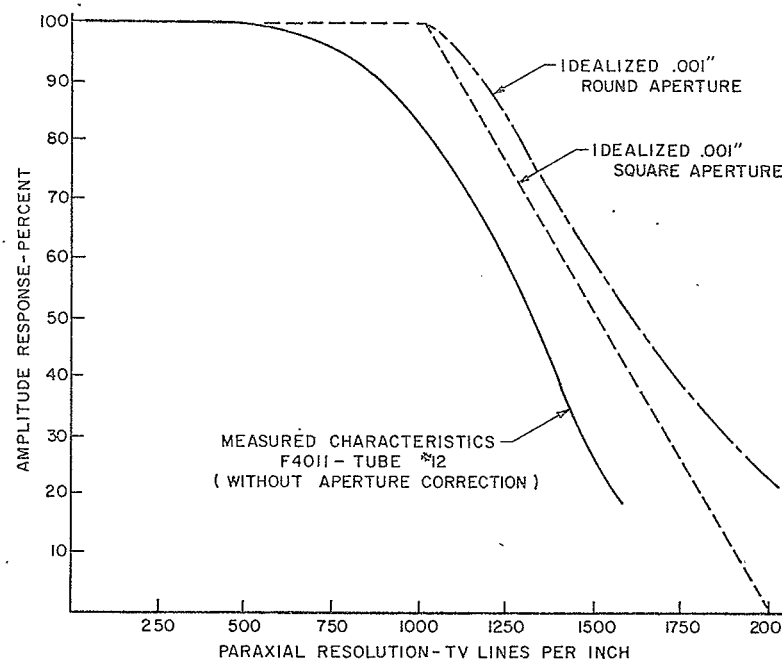

Figure 2 Resolution Characteristics

Outline Drawing

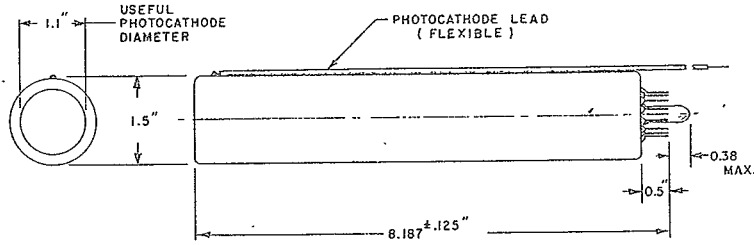

Pin Connections and Basing Diagram

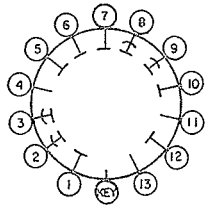

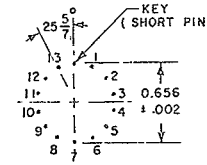

Pin 1 Anode	Pin 9 Dynode No. 2
Pin 2 Dynode No. 10	Pin 10 Drift Tube (DT)
Pin 3 Dynode No. 9	Pin 11 NC
Pin 4 NC	Pin 12 Shield
Pin 5 IC to DT	Pin 13 NC
Pin 6 IC to DT	Key NC (Short Pin)
Pin 7 IC to DT	Flying Lead Photocathode
Pin 8 Dynode No. 1	

IC - Internally Connected
NC - No Connection

Note: Pins 11 and 13 are internally connected to the drift tube in the F4011 (S-20).

Appendix B

SIGNAL-TO-NOISE RATIOS FOR UV IMAGERY

Appendix B1 provides examples of simulated UV imagery within the range of signal-to-noise ratios expected for Earth and lunar orbital imagery. These figures were obtained by viewing a high resolution photograph of Meteor Crater (Arizona), with a 400 line closed loop television system. Measured random noise was introduced into the display. The signal-to-noise ratios are defined here as the ratios of the square of the r.m.s values of signal and noise.

In Earth orbit an overall gray contribution from the atmosphere is expected. This component, provided it is uniform over (at least) one frame of imagery, can easily be removed from the final imagery by simple enhancement techniques. However the presence of such a contribution does increase the requirements on the system S/N ratio since it effectively compresses the gray scale intervals in the image.

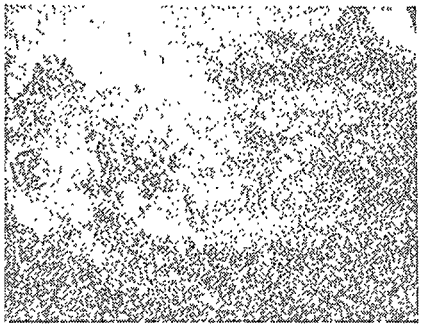

$S/_N = 1$

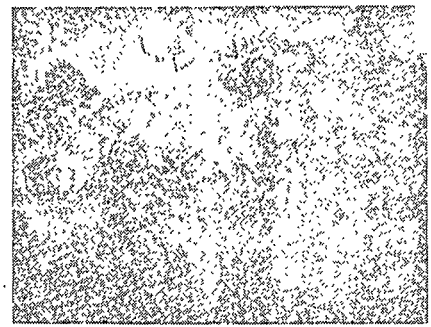

$S/_N = 10$

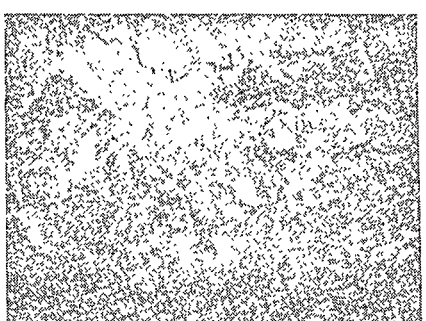

$S/_N = 100$

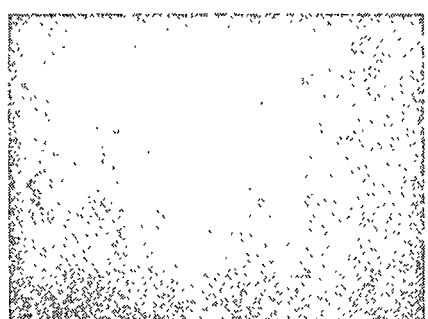

$S/_N = 400$
(WITH ADDED UNIFORM GRAY COMPONENT)

SIMULATED LINE SCAN IMAGERY OF METEOR CRATER FOR A RANGE OF SIGNAL/NOISE RATIOS.

Appendix B-1